EARLY-STAGE COUPLING FOR OBLIQUE IMPACTS IN GRANULAR MATERIAL B. Hermalyn[1], P.H. Schultz[1], and J.T. Heineck[2],[1]Brown University, Providence, RI 02912-1846 (Brendan_Hermalyn@brown.edu), [2]NASA Ames Research Center, Moffett Field, CA 94035

Introduction and Background: Impact events control the distribution of materials on planetary surfaces. Early-time processes, during which the projectile is still coupling its energy and momentum to the target, affect the emplacement of distal ejecta and play a greater role at larger planetary scales. These effects are especially apparent in oblique impacts, which often display early-stage asymmetries in the ejecta deposits. The early-time ejecta velocity distribution for oblique impacts has not been studied in detail for granular materials. Here we examine the time-resolved ejecta dynamics for oblique hypervelocity impacts through a novel imaging technique.

Background: Ejection velocities during main-stage excavation flow, when most material is ejected, have been well studied for vertical impacts in granular materials through dimensional analysis [1], numerical simulations [2], and experimental approaches [3, 4, 5, 6, 7, 8]. Such studies accommodate the predicted main-stage trend fairly well, consistent with the "late-stage equivalence" assumption for crater growth [9], where the details of the impact, i.e., the energy and momentum transfer of the projectile to the target, can be replaced by a singular point in time and space (e.g., [10, 11, 1]). While the projectile is still transferring its energy and momentum to the target at early times, however, the single power-law relationship does not hold [8]. Asymmetries in the initial shock from oblique impacts are manifested through azimuthally dependent velocities and ejection angles in the ejecta flow-field, persisting well into crater growth. The transition in flow regimes for oblique impacts extends well after that for a comparable vertical impact [7, 14, 15]. Previous studies have examined oblique ejecta distributions from the ballistic deposition of material on the surface (e.g., [16]), but little experimental data exists for the ejecta velocity distribution from oblique impacts early in the cratering process due to the difficulty of in-flight measurement of the three-dimensional nature of the flow field.

Experimental Methodology: In order to address and constrain the effects of oblique impact conditions on the early-time ejecta distribution, a suite of impact experiments into #20-30 sand (nominal grain diameter of $\sim 400\mu m$) was carried out at the NASA Ames Vertical Gun Range (AVGR). The strategy involved: varying impact angle (30°, 45°, 60°, 90°), speed (from ∼1km/s to 5.5km/s), projectile size (3.175mm to 12.7mm), and projectile density (factor of ~ 10). For this study, a technique based on high-speed 3-Component Particle Imaging Velocimetry (3C-PIV) was developed to measure the ejection velocity of the ejecta curtain in the experiments. Particle imaging velocimetry is a non-intrusive imaging technique capable of determining the velocity of in-flight ejecta over all azimuths. The 3C-PIV system utilizes a pulsed laser light sheet projected parallel to the impact surface to illuminate horizontal slices of the ejecta curtain (see Fig.1), which are then recorded by cameras. Cross-correlation between successive frames and cameras allows determination of displacement, and thus the three-component velocity, of the ejecta curtain. Pioneering PIV efforts [7, 14, 15] characterized the main-stage ejecta velocity distributions for a range of impacts into sand, and have demonstrated that asymmetries in velocity and ejection angle persist well into the far-field for oblique impacts. These studies focused on a single discrete pair of stereo images per impact experiment (i.e. one velocity vs. time "data point" per experiment); thus multiple identical experiments were required to collect sufficient velocity data for a specific impact condition. Extension of the PIV system to the high-speed technique necessary for studying the early-time dynamics requires fundamental changes to overcome new technical barriers. The new system developed at the AVGR for this application is called "High-Speed Over-Resolved 3-Component PIV," and uses mul-

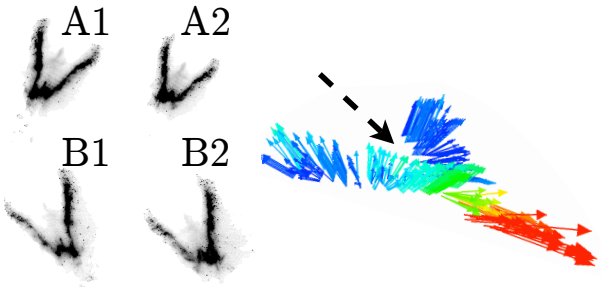

Figure 1: 3-C PIV Data Set. Multiple stereo pairs of imaged cross-sectional "slices" of the ejecta curtain (left) are cross correlated to find the displacements of individual particles. When coupled with the time between successive image pairs and the geometry of the cameras, the instantaneous three-component velocity of the ejecta can be measured. Images (inverted) are of a ∼1km/s 6.35mm Al projectile at 30° into sand. Vector plot (left) of post-processed data in the laser plane shows enhanced velocities in the downrange direction. Arrow indicates impact direction.

tiple high-speed cameras to image the same area (in this case, at 10,000 to 12,000 frames per second, or fps) from multiple viewpoints. A new software package performs cross-correlation between each set of cameras, thereby yielding an over-resolved system of displacement vectors for each interrogation area. The time-resolved nature of the data set allows investigation of the ejecta flow field in a regime much earlier than prior experimental or dimensional analysis.

Results and Analysis: In order to examine the ejecta dynamics for oblique impacts, we divide the expanding ejecta curtain into three components: uprange, downrange, and lateral to the direction of impact. The preliminary results of a 30° hypervelocity impact of a 6.35mm pyrex projectile into #20-30 sand are presented here. Ejection angles (Fig. 2) are asymmetric throughout the measurement of crater growth, and are not constant with time. The downrange component of ejecta initially has the lowest ejection angle. Further analysis of the PIV data will allow measurement of this component earlier in crater growth, where it qualitatively exhibits even lower initial ejection angles. Early-time uprange ejecta is very sparse; once the curtain fully closes, the uprange component exhibits a higher angle of ejection than the lateral or downrange regions. Velocities are similarly affected by the obliquity of impact. The downrange component demonstrates a clear velocity bias throughout much of crater evolution. Uprange ejecta arrives later than either downrange or lateral components, and is much slower when it does come into the laser plane. All three components approach the same velocity trend towards the end of crater growth, as seen by [7].

Conclusions and Implications: The new 3-C PIV technique developed allows investigation of the early-stage ejecta velocity distribution with a high degree of temporal resolution. In the downrange direction, an enhancement of high speed material early in the process is measured (e.g. [17, 18]), driven by the momentum of the projectile. In the uprange azimuth, incomplete coupling at early times forms the "zone of avoidance." The convolution of the decreasing ejection velocities and coupling time leads to the appearance of "curved" rays in the uprange direction [19]. Further study of the effect of different impact variables will constrain the early-time component and ultimately allow scaling to planetary events. With increasing crater size, early-time processes encompass a greater percentage of crater growth [12]. Understanding the evolution of the ejecta distribution is essential for interpretation of impact mission results (such as the Deep Impact mission) and the cratering record on planetary bodies.

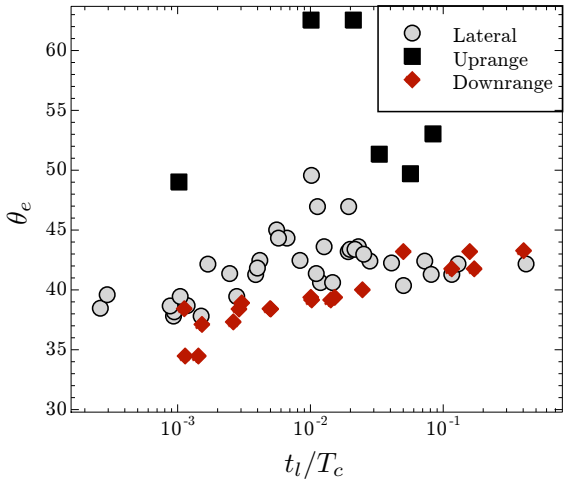

Figure 2: Ejection Angle Vs. Time Time after impact is scaled to the time of crater formation. Data is for a 30° impact of a 6.35mm pyrex projectile into sand at ~ 5.3km/s. Azimuth directions are with respect to the impact trajectory, and are binned in 15° increments.

References:

[1] Housen, K.R., *et al.* (1983) *JGR 88*.
[2] Wada, K., *et al.* (2006) *Icarus 180*(2). 528-545.
[3] Piekutowski, A.J. (1980) in *LPSC* XI. 877-878.
[4] Oberbeck, V.R., *LPSC Proceedings* VII. 2983-3005.
[5] Piekutowski, A.J.,(1977) *SPIE* vol. 97.
[6] Cintala, M.J., *et al.* (1999) *MAPS 34*. 605-623.
[7] Anderson, J.L.B., *et al.* (2003) *JGR(Planets) 108*.
[8] Hermalyn, B., *et al.* (2009) in *LPSC* XXXX. 2492.
[9] Dienes, J.K., Walsh, J.M. (1970) *High-Velocity Impact Phenomena*. 45-104.
[10] Chabai, A. (1959) *Tech. rep. SC-4391*.
[11] Orphal, D.L. (1977) *Impact and Explosion Cratering*. 907-917.
[12] Schultz, P.H. (1992) *JGR 97*.
[13] Dahl, J.M., Schultz, P.H. (2001) *IJIE 26*. 145-155.
[14] Anderson, J.L.B.,*et al.* (2004) *MAPS 39*(2). 303-320.
[15] Anderson, J.L.B., Schultz, P.H. (2006) *IJIE 33*. 35 - 44.
[16] Gault, D.E., Wedekind, J.A. (1978) in *LPSC* IX. 3843-3875.
[17] Schultz, P.H. (1999) in *LPSC* XXX. 1919.
[18] Schultz, P.H., Mustard, J.F. (2004) *JGR(Planets) 109*.
[19] Schultz, P.H., *et al.* (2009) in *LPSC* XXXX. 2496.